

Supporting Information

Photo-modulation of 2D-Self-assembly of Azobenzene-Hexa-*peri*-hexabenzocoronene-Azobenzene Triads

Ian Cheng-Yi Hou,¹ Valentin Diez-Cabanes,² Agostino Galanti,³ Michal Valášek,⁴ Marcel Mayor,^{4,5} Jérôme Cornil,² Akimitsu Narita,^{1,*} Paolo Samori^{3,*} and Klaus Müllen^{1,6,*}

¹Max Planck Institute for Polymer Research, Ackermannweg 10, D-55128 Mainz, Germany

²Laboratory for Chemistry of Novel Materials, University of Mons, Place du Parc 20, B-7000 Mons, Belgium

³Université de Strasbourg, CNRS, ISIS UMR 7006, 8 allée Gaspard Monge, 67000 Strasbourg, France

⁴Karlsruhe Institute of Technology KIT, Institute for Nanotechnology, P.O. Box 3640, 76021 Karlsruhe, Germany

⁵Department of Chemistry, University of Basel, St. Johannisring 19, 4056 Basel, Switzerland

⁶Institute of Physical Chemistry, Johannes Gutenberg-University Mainz, Duesbergweg 10-14, D-55128 Mainz, Germany

Table of contents

1. Experimental details.....	S2
2. UV-Vis absorption spectra Figure S1, S2, S3 and ¹ H NMR spectra S4.....	S4
3. STM images Figure S5, S6 and the summarized table S1.....	S6
4. MM/MD simulation results Figure S7 and Table S2.....	S8
5. ¹ H NMR and ¹³ C NMR spectra Figure S8 and S9 of <i>p</i> AHA and <i>o</i> AHA.....	S11
6. References.....	S13

1. Experimental details

Photoswitching in solution

Solution used were heated at 80 °C overnight prior to investigation to ensure that all molecules were in *E*-form. The 365 nm light irradiation was achieved by using a 3 mm GG320 combined with a UG11 filter to eliminate the high energy UV peaks and the visible light peaks of the light source to reveal only the 366 nm peak ($P_d = 70 \text{ mW cm}^{-2}$). The 436 nm light irradiation was achieved by using 3 mm GG395 filter to block the UV light from the light source ($P_d = 310 \text{ mW cm}^{-2}$). Lower energy peaks of the light source were not blocked. The experiments were conducted at room temperature. If not specified, the irradiation interval was 10 s. The light source used for the photoisomerization in THF- d_8 for tracking the reaction by ^1H NMR spectra is the same for UV-Vis measurement. Because the solution is 100-times more concentrated than that for UV-Vis experiments, as well as the partial absorption of 366 nm light by the NMR tube (glass), the irradiation time was longer.

STM investigation

The surface of the HOPG substrate was peeled off (Scotch tape) several times until visually flat before use. Solution used were heated at 80 °C overnight before investigation to ensure all materials were in *E*-form. At the concentration used for investigation, the materials will eventually slowly precipitate out from the solution because of strong intermolecular π - π stacking. Nevertheless, the molecule-substrate interaction still overcome the intermolecular stacking and the 2D supramolecular self-assembly pattern was observed.

MM/MD simulations

Following the reported methodologies^{1,2}, an orthorhombic unit cell of dimensions $a = 487\text{\AA}$, $b = 324\text{\AA}$ and $c = 50\text{\AA}$ coupled to Periodic Boundary Conditions (PBC) was used to reproduce structural packing of the graphene substrate. This graphene layer has been considered as an infinite rigid body to reduce the computational cost. In this unit cell, a self-assembly group of 144 molecules (12 rows and columns) was placed on the graphene substrate, whereas the big dimensions of the unit cell ensure a large lateral vacuum distance ($>40\text{\AA}$) between the replicated group of molecules. The simulation have been carried out in vacuum following the NVT ensemble (constant number of particles, volume and temperature) with a temperature of $T=100\text{K}$. The thermostat used to monitor the temperature was Velocity Scale. The atomic charges were calculated following the Gasteiger method,³ while a cut-off distance of 12.5\AA was used in the non-bonded interactions. Firstly, the unit cell was optimized at MM level. The resulting optimized unit cell was used as starting point for the quenched simulation (MM/MD). The run simulation time used was 25 ps, whereas the time step was 1 fs. The geometries of the MM/MD run were extracted every 500 steps, thus resulting in a total of 50 geometries per run. The geometry with lower energy was used as starting point for a new quenched simulation. All this process has been repeated till the energy difference between the starting and the most stable geometry is very low.

Some of the assumptions used in our model are: (i) the 2D self-assembly is formed by one single layer of HBC monomers, all of them made of a single isomer (*E,E*; *E,Z* or *Z,Z*); (ii) all alkyl chains of the HBC compounds are adsorbed on the graphite layer, implying that all atoms of the alkyl chains are in the same plane as the HBC core; and (iii) only the best fitting models which ended up in clear self-assembled pattern from several starting models have been shown here ; our models thus represent one of the possible suitable patterns with similar structural parameters as the STM images.

In order to obtain a more complete interpretation of the experimental findings, we casted down the different energies driving the 2D self-assembly of the two HBC compounds on graphite. For this purpose, we have computed two parameters: adsorption energy (E_{ads}) and binding energy (BE), giving us a hint on the relative strength of the molecule-substrate and molecule-molecule interactions. The adsorption energy (E_{ads}) has been computed as the average adsorption energy of an individual HBC molecule on the graphite surface, following eq. 1:

$$E_{ads} = \frac{E_{tot} - E_{Gr} - E_{HBC}}{n} \quad (1)$$

With E_{tot} the total energy of the system, E_{Gr} the energy of the graphite layer, E_{HBC} the energy of the monolayer of HBC molecules and n the number of HBC molecules that form the assembly. In our case we have taken $n = 64$. The binding energy (BE) has been defined as the average interaction energy between HBC molecules in the assembly following eq. 2:

$$BE = \frac{E_{HBC} - \sum_{i=1}^n E_i}{n} \quad (2)$$

With E_i the energy of the individual molecules that form the monolayer. As in the last case we considered a representative assembly made of 64 molecules. These energies are also collected in Table S2.

2. UV-Vis absorption spectra Figure S1, S2, S3 and ^1H NMR spectra Figure S4

Figure S1. UV-Vis absorption spectra of the THF solutions of (a) **pAHA** (9.1×10^{-6} M) and (b) **oAHA** (1.3×10^{-5} M) without light irradiation (*black line*) and at the PSS of 366 nm irradiation (*red line*). Arrows show the trend of the spectral change at different spectral region.

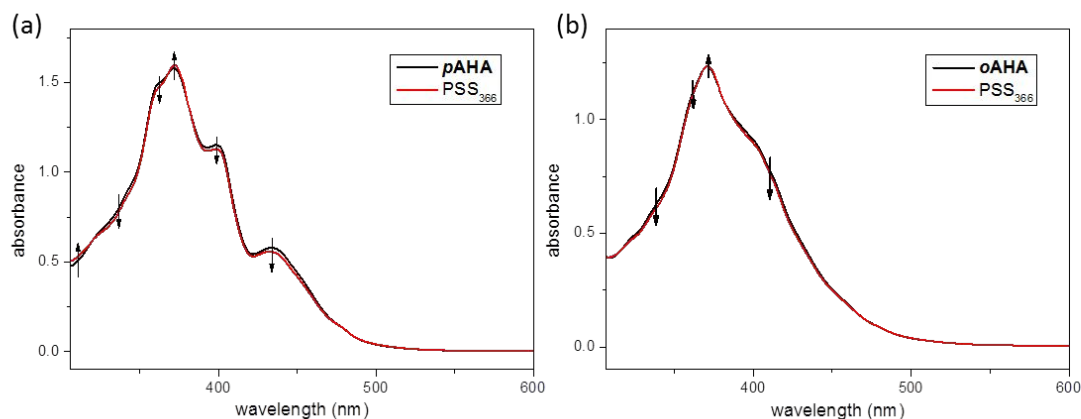


Figure S2. Absorbance variation of (a) **pAHA** (4.5×10^{-7} M) and (b) **oAHA** (1.3×10^{-6} M) in THF monitored at 368 nm starting from PSS₃₆₆ upon alternated irradiation with 436 and 366 nm light.

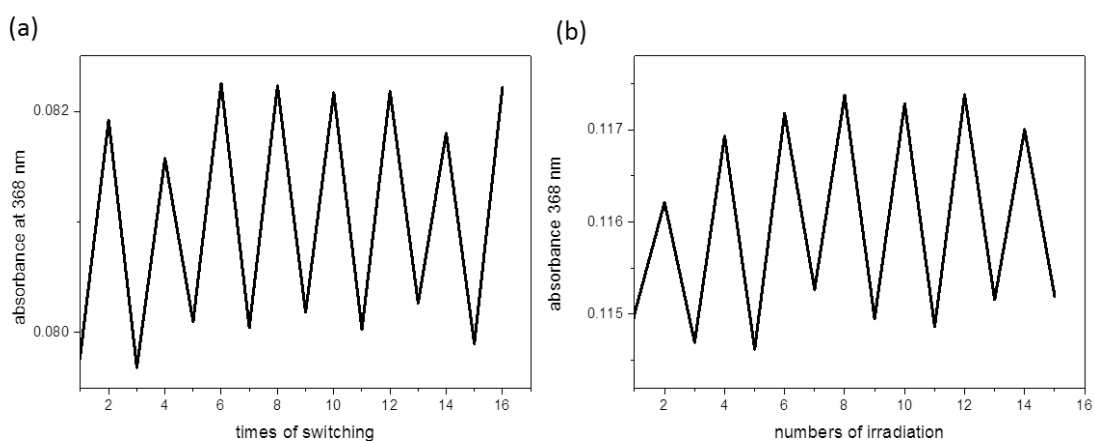


Figure S3. UV-Vis absorption spectra of (a) **pAHA** (4.5×10^{-7} M) and (b) **oAHA** (1.3×10^{-6} M) in THF after the first cycle and the seventh cycle of photoswitching.

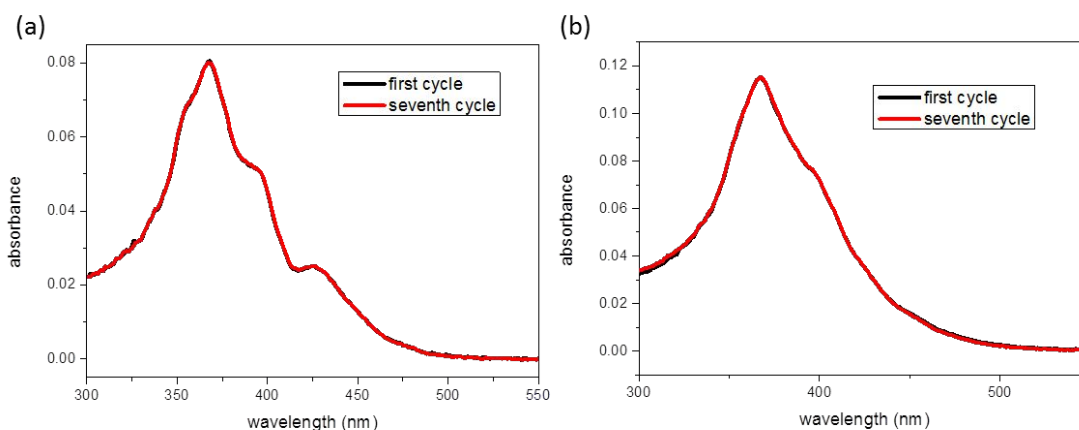
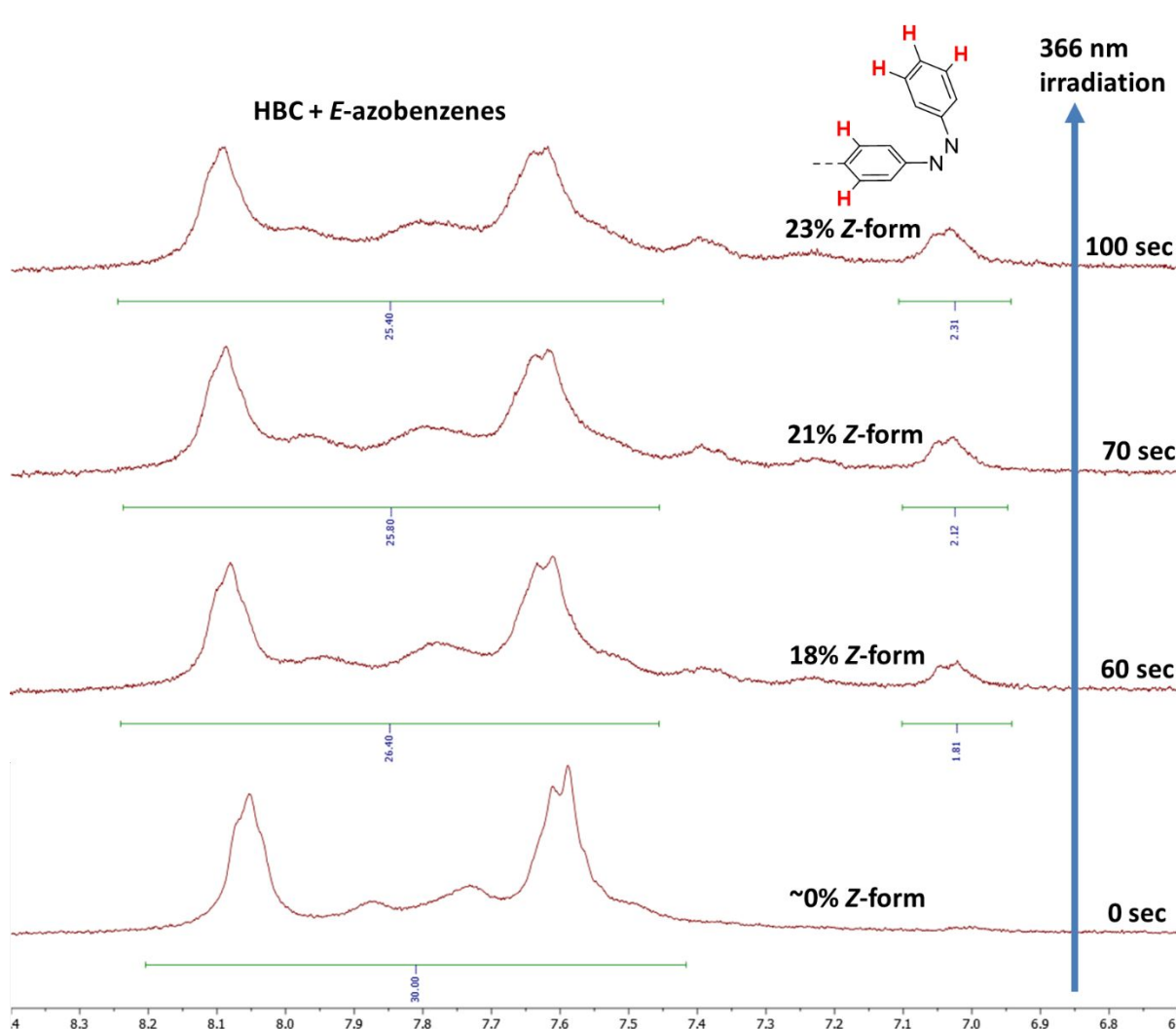


Figure S4. Aromatic region of the ^1H NMR spectra of **oAHA** in THF-d_8 recorded after different time of direct irradiation of the solution in NMR tube with 366 nm light until the PSS was reached. The broad peak at around 6.95–7.10 ppm is assigned to the signals of the protons of Z-azobenzene labeled in red. The integration of this peak is compared with the integration of the protons on HBC and *E*-azobenzene (7.15–7.45 ppm) to estimate the percentage of photoisomerization. An integration of 10 protons (2 azobenzenes) corresponds to 100% of Z-form. Note that the rest of the signals of Z-azobenzene appear at around 7.15–7.45 ppm. The broadening and shifting of the signal around 7.4–8.2 ppm is an indication of changing of the aggregation of HBCs caused by variation of the composition of isomers.



3. STM images Figure S5, S6 and the summarized Table S1

Figure S5. STM images recorded at the interface of HOPG and a 0.1 mM TCB solution of ***o*AHA**. The image corresponds to ***o*AHA** *ori2* in Table S1. Inset: the same crystal packing taken in a larger area of 50 nm × 50 nm. Tunneling parameters: $V_T = -750$ mV, $I_T = 20$ pA.

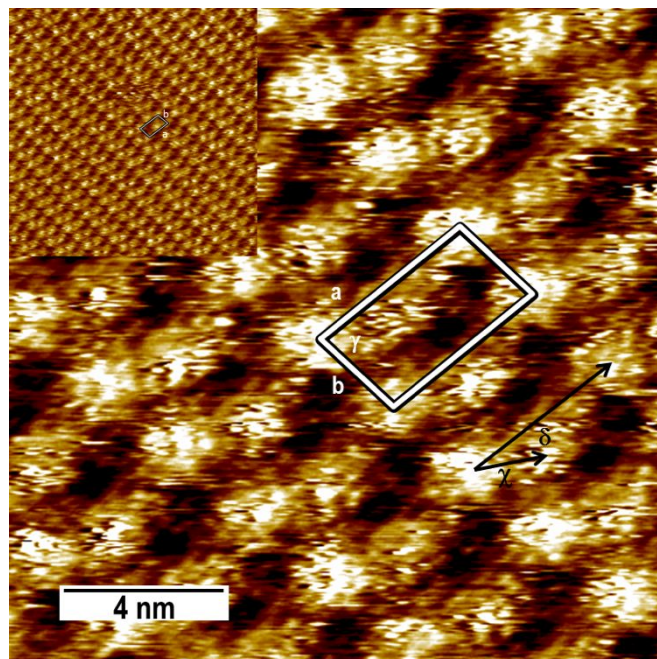


Figure S6. STM images recorded at the interface of HOPG and a 0.1 mM TCB solution of ***p*AHA** after irradiation with 366 nm light. The image corresponds to ***p*AHA** *irr2* in Table S1. Inset: the same crystal packing taken in larger area of 50 nm × 50 nm. The newly formed dimer row crystal packing is found coexist with the oblique packing formed before irradiation with a clear border as can be seen in the inset of (b). Tunneling parameters: $V_T = -300$ mV, $I_T = 20$ pA.

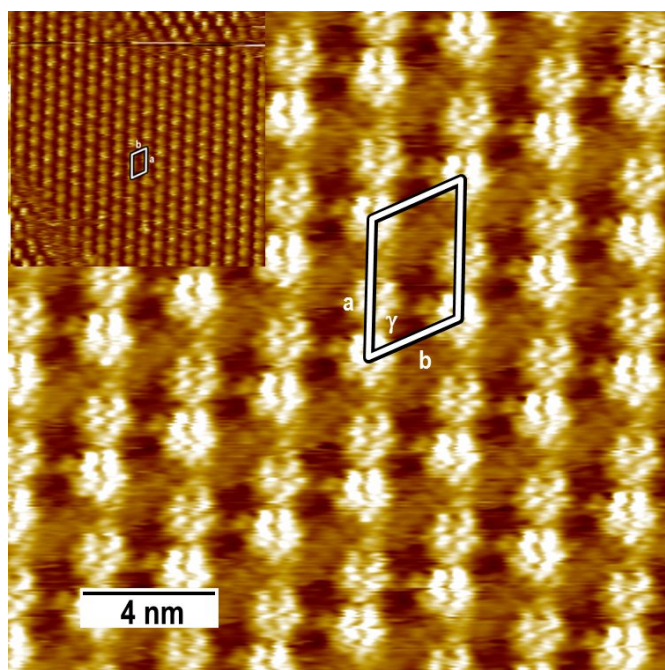


Table S1. Lattice constants of the additional experimental 2D crystal packing of **pAHA** and **oAHA**.

	a (nm)	b (nm)	γ (°)	χ (nm) ^b	δ (°) ^c	Area per molecule (nm ²)
pAHA <i>irr2</i> ^a	4.3 ± 0.2	3.00 ± 0.04	63 ± 2	1.74 ± 0.05	-0.1 ± 0.9	5.7 ± 0.3
oAHA <i>ori2</i>	4.3 ± 0.3	2.65 ± 0.08	80 ± 4	2.4 ± 0.2	17 ± 4	5.6 ± 0.4

^aOnly formed after 366 nm light irradiation. ^bThe inter-row distance, specified in the STM Figures. ^cThe inter-row angle, specified in the STM Figures.

4. MM/MD simulations results Figure S7 and Table S2

The adsorption energies E_{ads} of both E,Z and Z,Z present lower energy values respect to the E,E isomer (~ 5 kcal/mol for E,Z and ~ 15 kcal/mol for Z,Z) due to the lower π - π interactions caused by the non-planar configuration of the Z -form. However, due to the large aromaticity of the HBC, the magnitude of E_{ads} is one order of magnitude higher than BE . As a consequence, this factor is dominating the assembly process, thus explaining the highly packed patterns observed in the STM images.

In the case of the binding energy BE , comparing first this energy among the two structural models of **pAHA** for the E,E form, it is found that model II presents an energy twice higher than model I, thus demonstrating the importance of alkyl chains interdigitation in the intermolecular stabilization. Nevertheless, in most of the cases BE increases with the number of Z units, thus showing that the intermolecular interactions help to stabilize the Z -forms within the assembly.

Figure S7. Summary of the STM images of ordered domains of **pAHA** found (a) before and (b)(c) after the 366 nm irradiation; and **oAHA** found (d) before and (e) after the 366 nm irradiation. Right side: corresponding supramolecular packing models of various isomers obtained by MM/MD simulations for each STM pattern on the left sides.

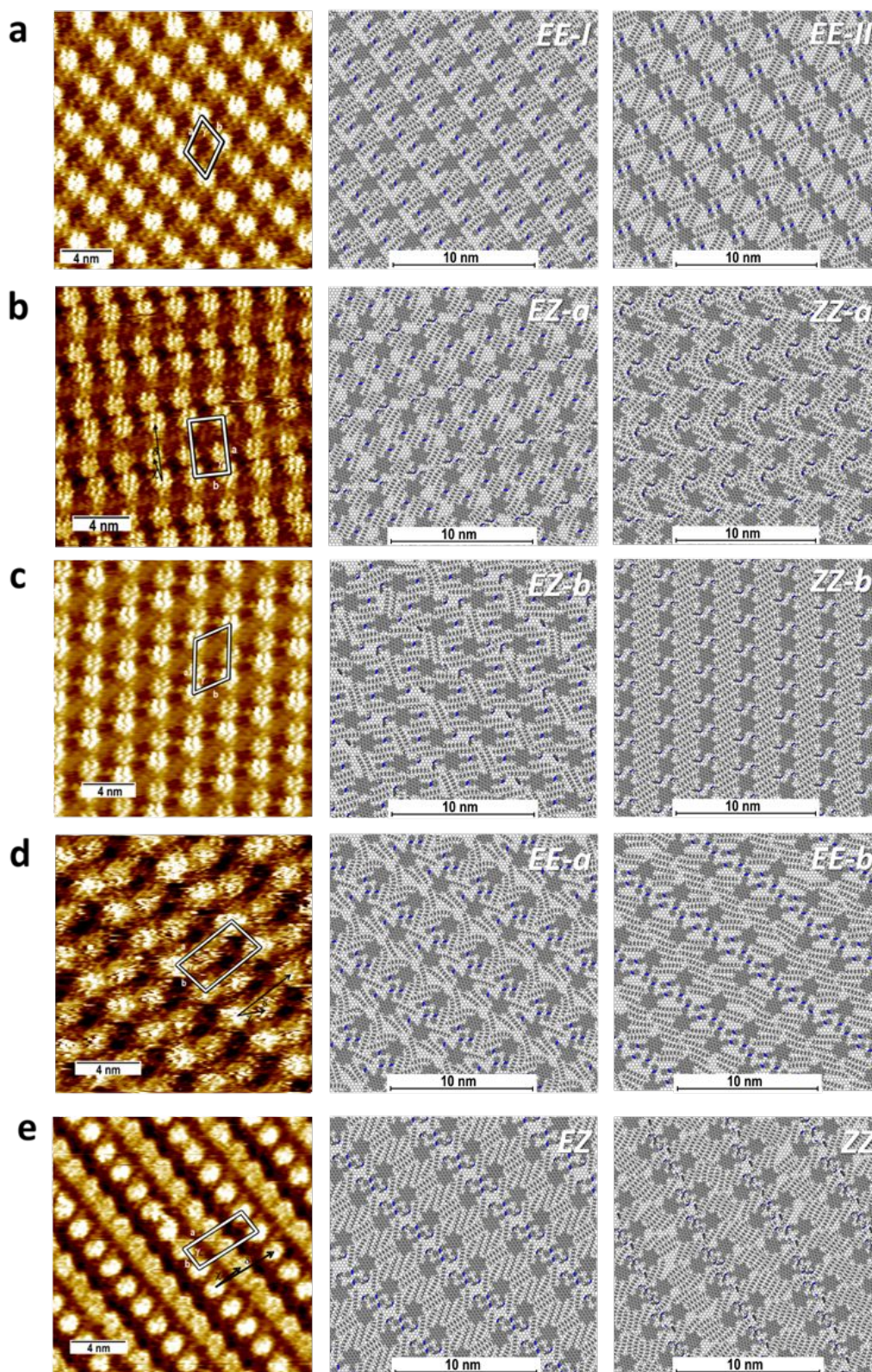


Table S2. Experimental (*ori*- for original and *irr*- for irradiated) and theoretical unit cell parameters (lateral dimensions *a* and *b*, corresponding angle γ , area occupied per molecule *A*, center to center distance χ between non-equivalent molecules in the unit cell and angle δ formed by the vector connecting the non-equivalent molecules and the *b* lateral vector) and calculated thermodynamic quantities (adsorption (E_{ads}) and binding (*BE*) energies). The highlighted rows are used to help making a direct comparison between the experimental (numbers in parentheses) and the best fitting theoretical models. Only the first model is formed by one molecule in the unit cell while the rest of the models are composed by two molecules in the unit cell.

<i>HBC</i>	<i>Model</i>	<i>a</i> (nm)	<i>b</i> (nm)	γ (°)	<i>A</i> (nm ²)	χ (nm)	δ (°)	E_{ads} (kcal/mol)	<i>BE</i> (kcal/mol)
<i>pAHA</i>	<i>ori</i>	(3.0)	(2.5)	(65)	(6.8)	-	-	-	-
	<i>EE-I</i>	3.0	2.5	64	6.8	-	-	-212.71	-11.09
	<i>EE-II</i>	3.2	2.5	62	6.9	-	-	-210.89	-23.35
	<i>irr</i>	(4.2)	(2.52)	(88)	(5.3)	(1.6)	(11)	-	-
	<i>EZ-a</i>	5.0	2.66	83	6.6	2.3	9.4	-204.57	-13.83
	<i>ZZ-a</i>	4.3	2.80	89	6.0	2.0	17	-195.99	-17.15
	<i>irr2</i>	(4.3)	(3.00)	(63)	(5.7)	(1.74)	(-0.1)	-	-
	<i>EZ-b</i>	4.6	3.10	62	6.3	1.80	22	-204.96	-17.13
	<i>ZZ-b</i>	4.1	3.18	62	5.7	2.04	0.1	-194.96	-24.36
	<i>ori</i>	(4.4)	(2.7)	(81)	(5.9)	(2.0)	(25)	-	-
<i>oAHA</i>	<i>EE-a</i>	4.9	2.8	79	6.7	2.4	24	-211.58	-17.27
	<i>ori2</i>	(4.3)	(2.65)	(80)	(5.6)	(2.4)	(17)	-	-
	<i>EE-b</i>	4.6	2.93	84	6.7	2.1	16	-208.47	-13.51
	<i>irr</i>	(5.2)	(1.77)	(83)	(4.6)	(2.4)	(-4)	-	-
	<i>EZ</i>	5.4	2.28	80	6.1	2.6	11	-205.72	-19.50
	<i>ZZ</i>	5.1	2.27	79	5.7	2.4	16	-192.53	-25.70

5. ^1H NMR and ^{13}C NMR APT spectra of *p*AHA and *o*AHA

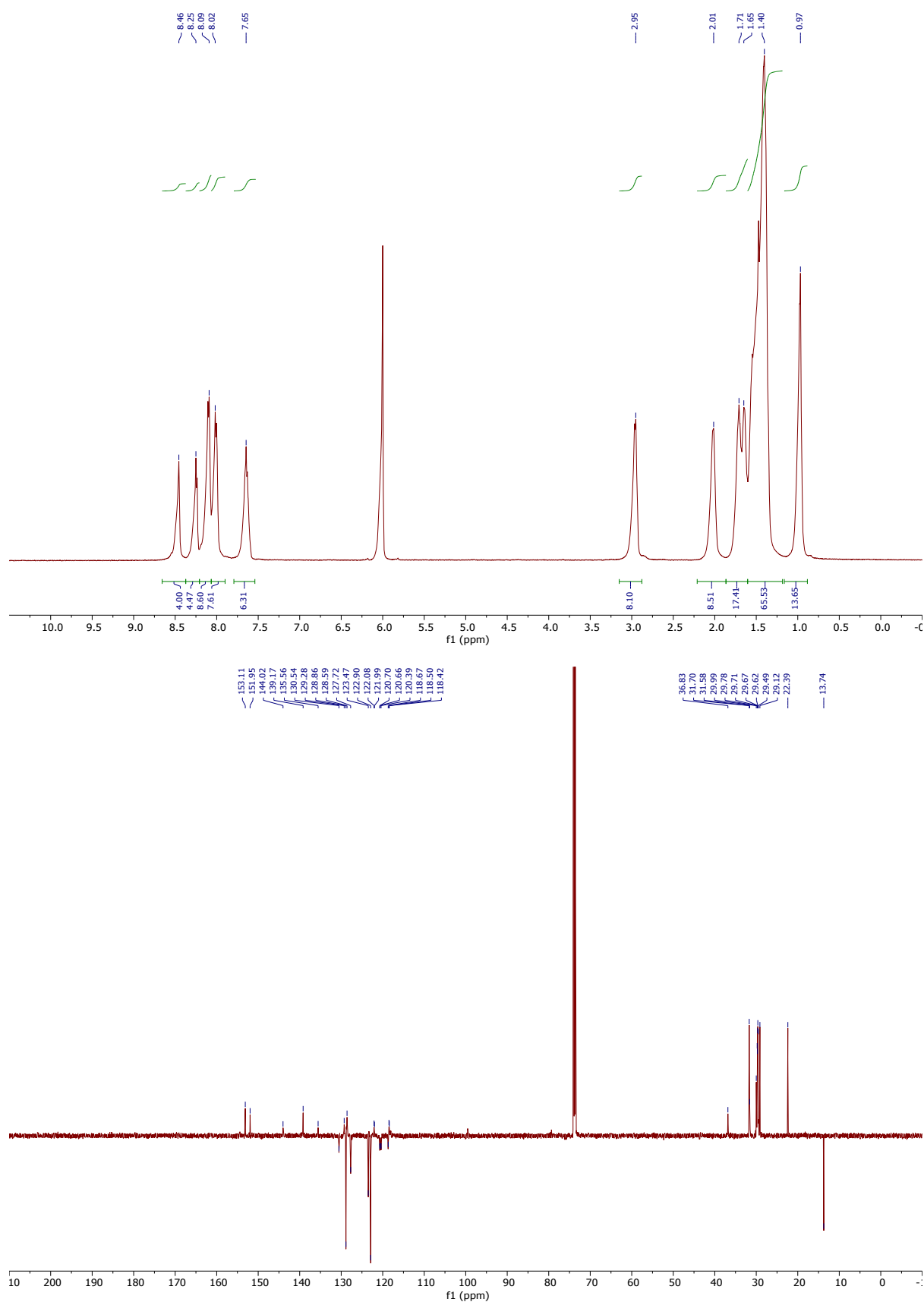


Figure S8. ^1H NMR (Up, 500 MHz, $\text{C}_2\text{D}_2\text{Cl}_4$, 373 K) and ^{13}C NMR APT spectra (Down, 126 MHz, $\text{C}_2\text{D}_2\text{Cl}_4$, 373 K) of *p*AHA.

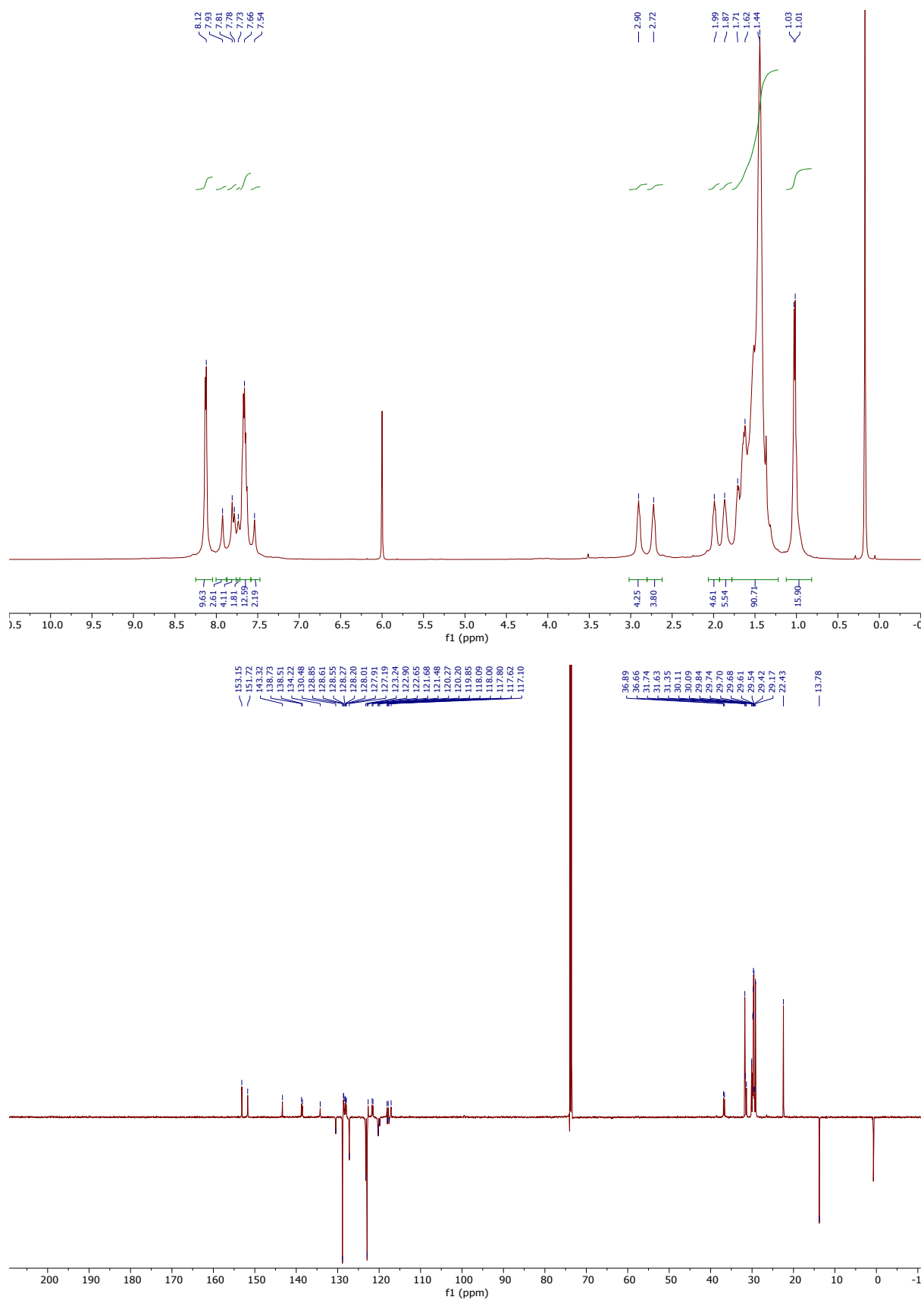


Figure S9. ¹H NMR (Up, 500 MHz, C₂D₂Cl₄, 373 K) and ¹³C NMR APT spectra (Down, 126 MHz, C₂D₂Cl₄, 373 K) of **oAHA**.

6. References

- (1) Galanti, A.; Diez-Cabanes, V.; Santoro, J.; Valášek, M.; Minoia, A.; Mayor, M.; Cornil, J.; Samorì, P. Electronic Decoupling in C₃-Symmetrical Light-Responsive Tris(Azobenzene) Scaffolds: Self-Assembly and Multiphotochromism. *J. Am. Chem. Soc.* **2018**, *140* (47), 16062–16070.
- (2) Mayo, S. L.; Olafson, B. D.; Jii, W. A. G.; Eb, E.; El, E. A. E. T. DREIDING: A Generic Force Field for Molecular Simulations. *J. Phys. Chem.* **1990**, *94* (26), 8897–8909.
- (3) Gasteiger, J.; Marsili, M. A New Model for Calculating Atomic Charges in Molecules. *Tetrahedron Lett.* **1978**, *19* (34), 3181–3184.
- (4) MS Modeling, V7. Accelrys Software Inc.: San Diego, CA 2015.